Distant synchronization through a passive medium

V. S. Petrov,[1] G. V. Osipov,[1] and J. Kurths[2,3,4]
[1]*Department of Control Theory, Nizhny Novgorod University, Gagarin Avenue 23, 603950 Nizhny Novgorod, Russia*
[2]*Institute for Complex Systems and Mathematical Biology, University of Aberdeen, Aberdeen AB24 3UE, United Kingdom*
[3]*Institute of Physics, Humboldt University Berlin, 12489 Berlin, Germany*
[4]*Potsdam Institute for Climate Impact Research, 14412 Potsdam, Germany*
(Received 18 June 2010; published 24 August 2010)

This paper deals with the phenomenon of synchronization of oscillatory ensembles interacting distantly through the passive medium. Main characteristics of such a kind of synchronization are studied. The results of this work can be applied to describe the synchronization of cardiac oscillatory cells separated by the passive fibroblasts. In this work the phenomenological models (Bonhoeffer–Van der Pol) of cardiac cells as well as biologically relevant (Luo-Rudy, Sachse) models are used. We also propose equivalent model of distant synchronization and derive on its basis an analytical scaling of the frequency of synchronous oscillations.

DOI: 10.1103/PhysRevE.82.026208 PACS number(s): 05.45.Xt

I. INTRODUCTION

Synchronization is one of the most important phenomena in science [1,2]. Numerous evidences confirm its presence in physics, chemistry, electrical engineering, neuroscience, biology, sociology etc. [3–5]. In the last decades synchronization has attracted lots of interest. Various kinds of synchronization were discovered, such as phase, complete, partial, generalized ones. There are also many works devoted to study of synchronization in specific systems and its applications [6,7]. Thus, for example, the synchronization in the heterogeneous medium of pancreatic β cells was studied in [8,9]. In this paper we focus on synchronization of oscillatory systems which are separated by a passive medium and thus interacting through it. This problem arises in various biological experiments, especially in cardiac cell cultures. It is worth saying that nowadays investigations in the sphere of heart functioning and cardiac dynamics are of the great importance [10]. In order to motivate our work we stop briefly at the structure of the heart. It consists of cells of different types. Among them there are three major cell types: pace making cells, excitable cells of working myocardium and fibroblasts. From the point of view of nonlinear dynamics these cells are oscillatory, excitable and passive elements, respectively [11]. Oscillatory cardiac cells form several pace making areas in the heart (sino-atrial node, atrio-ventricular node) that generate a sustainable rhythm and send an electrical stimulus to the working myocardium. It consists of excitable cells which, in turn, are able to contract when a stimulus from the pacemaker arrives. Excitable cells occupy the most part of the heart. But the largest number is held by fibroblasts. These cells for some time were considered as supporting units, but recent studies have shown that they play a much more important role in the regulation of the heart functioning [12].

In terms of nonlinear science the difference between excitable and passive elements is in the structure of their phase space. For the former element type the presence of a threshold manifold is necessary, while for the latter elements there has to be just a stable steady state. In this case any perturbation of a passive cell from its steady state would rapidly decrease and no action potential would be generated. On the other hand, a large enough perturbation to an excitable cell would move the phase point beyond the threshold manifold resulting in an action potential.

There are different ways to study cardiac dynamics: real experiments with the whole heart, cardiac cell cultures, ECG analysis, computer simulations etc. We use here the results of a real experiment as a motivation of our work. Namely, in [13] it has been recently considered a cardiac cell culture consisting of cells of only two types: fibroblasts and pacemakers. These cells were dissociated and plated on the Petri dish. Initially there were no oscillations in the system. After some time cells started to move and to form clusters of excitable cells separated by fibroblast medium. Later on, different excitable clusters have become oscillatory and started to oscillate with different individual frequencies. After that these clusters tended to synchronize until after some critical time the effect of complete synchronization between the oscillatory clusters had set in. The first effect observed in [13] showing that excitable cardiac cells may become oscillatory due to the interaction with passive fibroblasts was studied in several papers [14,15]. But for the last phenomenon of synchronization of oscillatory clusters through a passive medium there are no any theoretical studies yet. This effect is in the focus of the present work.

The paper consists of two parts: (i) theoretical studies of synchronization through the passive medium based on phenomenological models of cardiac cells and (ii) computer simulations with biologically relevant cardiac cell models validating the results obtained. Further in the paper we will refer to the synchronization of oscillatory units through a medium of passive cells as to distant synchronization (DS).

II. DS IN PHENOMENOLOGICAL MODEL OF CARDIAC CELLS

In this section we demonstrate the possibility of DS and study its properties using simple phenomenological models of cardiac cells. As a model of cardiac pace making cell we use the well-known Bonhoeffer–Van der Pol (BVdP) system [16], also called FitzHugh-Nagumo system [17].

$$\dot{x} = x - x^3/3 - y,$$

$$\dot{y} = \varepsilon(x + a). \tag{1}$$

Despite its simplicity the model reproduces the main peculiarities of cardiac cells, namely, the generation of action potential. This model may behave as an excitable or oscillatory cell according to the value of the parameter a. Since we are interested in the synchronization properties in the system, we do not pay attention to the transition of a cardiac cell from excitable to oscillatory state and use BVdP elements in the latter regime. The parameter a in this case may vary within the interval $(-1;1)$. Note that different values of a correspond to different individual frequencies of the BVdP element. As for the fibroblasts we use a simple first order linear kinetics to describe dynamics of the passive element.

$$\dot{x} = -\alpha(x - P). \tag{2}$$

This is an appropriate simplification as argued in [18]. We consider a more general case of a complex nonlinear description of cardiac cells in the second part of the paper. In Eq. (2) P describes the steady state of the passive element and has the notation of the fibroblast resting potential. The parameter α is responsible for the rate of convergence to the steady state. Its value should be chosen from biological considerations. In the heart the characteristic time scale of a fibroblast is half the period of the oscillation of the pace making cell. This means that on this time scale the amplitude of fibroblast voltage decreases from the maximal value of the pacemaker action potential to its steady state. In case of BVdP system this time scale may be estimated which gives the value of α about 0.02. This value is used in our simulations unless another is specified. The value of ε equals 0.01.

A. Dynamical properties of the passive medium

In this subsection we investigate how the signal generated by the oscillatory BVdP element propagates through the passive medium. We consider a chain of $N=11$ elements where only the first one is a BVdP in an oscillatory regime and the rest are passive. All elements are coupled diffusively via the variable x,

$$\dot{x}_1 = x_1 - x_1^3/3 - y_1 + d(x_2 - x_1),$$

$$\dot{y}_1 = \varepsilon(x_1 + a_1),$$

$$\dot{x}_i = -\alpha(x_i - P) + d(x_{i-1} - 2x_i + x_{i+1}),$$

$$i = 2,N, \quad x_{N+1} = x_N. \tag{3}$$

In the simulations the value of a_1 was set to zero with no loss of generality. Apart from it, it is easy to see that the linear transformation of the coordinates $x_i^* = x_i - P$, $i=2,N$, $y_1^* = y_1 - dP$, $x_1^* = x_1$ eliminates P from system [Eq. (3)]. So we can consider it to be equal zero.

Figure 1(a) shows the amplitudes A_i of oscillations of the elements in the chain for fixed values $d=0.4;0.2;0.1$ (curves with square, circle, and triangle markers, respectively). The

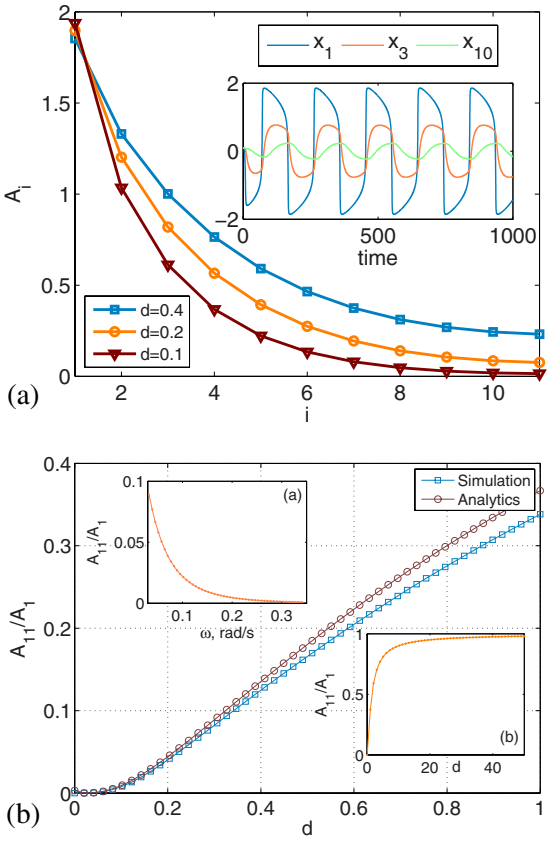

FIG. 1. (Color online) (a) The distribution of oscillation amplitudes over the chain for a fixed value of coupling $d=0.4;0.2;0.1$ (square, circle, and triangle curves). Inset shows the characteristic time series of the elements with numbers $i=1,3,10$ (the trace with the smaller amplitude corresponds to the larger number). (b) Analytical (circle curve) and numerical (square curve) dependence of the oscillation amplitude of the last passive element A_{11} related to that of the first oscillatory element A_1 on the coupling d. In the inset (a) there is a dependence of A_{11}/A_1 on the frequency of oscillations obtained analytically. Inset (b) shows saturation of A_{11}/A_1 for extremely large coupling.

amplitudes are defined as the differences between the maximum and minimum values of the time series of the corresponding element after some transients. One can see that the amplitude decreases drastically with the increase of the distance between the element with the number $i \geq 2$ and the only oscillatory element ($i=1$). In other words for every chosen value of the coupling strength d there exists a critical distance of signal propagation through the passive medium. Suppose that there is another oscillatory element on the other side of the chain. Then there exists some critical distance between the oscillators when they start to interact. On the other hand if the chain length (distance between the oscillatory elements) is fixed then the role of the critical parameter is played by the coupling d. The inset in Fig. 1(a) demonstrates the time series for the elements with the numbers $i=1,3,10$. Figure 1(b) illustrates the relation A_{11}/A_1 between the amplitudes of the last and the first element of the chain depending on d. The curve with square markers was obtained using computer simulations and represents the nonlinear increase of the amplitude in the last element for growing d. We

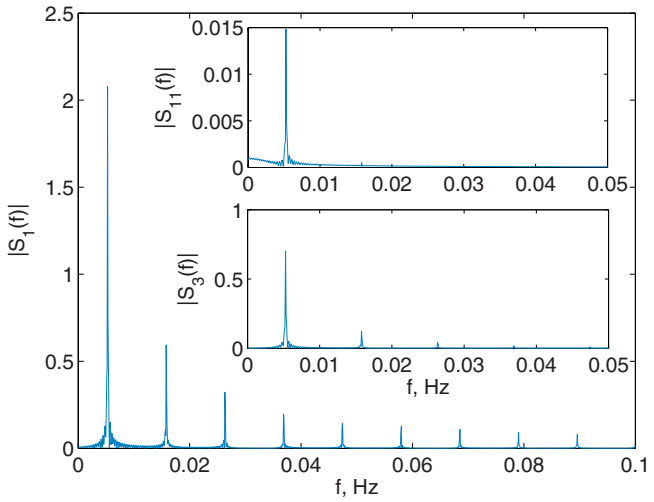

FIG. 2. (Color online) Power spectrum of the x variable time series of the elements of the chain obtained by fast Fourier transform for $d=0.1$. Lower and upper insets show power spectrum of the third and last elements of the chain, respectively.

will use this dependence further for the description of synchronization in the chain.

Amplitude relations of the propagating signal are important. However, spectrum properties for complex signals should be also taken into account. If the signal is harmonic then it will produce a harmonic response on the same frequency in the passive medium due to its linearity. But if the signal is more complex then each Fourier component may propagate differently resulting in a modification of the spectrum. Figure 2 represents the power spectrum of the time series of the x variable (corresponding to the voltage in real cells) of oscillatory BVdP element for $d=0.1$. It is clear that along with the major peak at the low-frequency of the periodic oscillations of the x variable there are also several other peaks at the higher frequencies that appear because of the nonlinearity in the system. The insets in Fig. 2 show the transformations of this spectrum, while it propagates through the passive medium. The lower inset corresponds to the third element in the chain. One can see that most higher harmonics have already vanished at this rather short distance from the source (note two times shorter scale on the x-axes). The spectrum of the last element in the chain (upper inset in Fig. 2) has the only peak at the frequency of the periodic oscillations of oscillatory BVdP element. Summing up the results obtained we find that the nonlinear oscillations of BVdP element on the left side of the chain produce a nearly harmonic low-amplitude signal on the other side of the chain as the output. With the increase of d the amplitude of the output and the degree of nonlinearity increase.

Next, we present some analytical descriptions of the observed effect. We describe the chain of passive elements with one oscillatory element at the beginning by the following partial differential equation with nonstationary boundary conditions:

$$\frac{\partial U}{\partial t} = -\alpha U + D\frac{\partial^2 U}{\partial x^2},$$

$$U(0,t) = A\,\sin(\omega t), \quad \left.\frac{\partial U(x,t)}{\partial x}\right|_{x=L} = 0,$$

$$U(x,0) = 0, \tag{4}$$

where L is the string length. This equation is a continuous analog of the chain that we considered previously. Here $U(x,t)$ has the meaning of the voltage of cardiac cell, i.e., it stands for the x variable of system [Eq. (3)]; x—is the space coordinate; $D\partial^2 U/\partial x^2$ describes the diffusion in the system. If we have a solution $U(x,t)$ of Eq. (4), we can approximate it to the chain with elements number N and coupling d assuming: $L=1$, $h=1/(N-1)$, $D=dh^2$, where h is the discretization step. The boundary condition on the left side of the string is a harmonic force with the frequency ω and amplitude A. Due to the linearity of the medium any complex signal will propagate as a superposition of its Fourier harmonics. Using Eq. (4) we can analyze how these harmonics propagate through the passive medium. The solution of Eq. (4) is given by

$$U(x,t) = A\,\sin(\omega t) - \frac{4A}{\pi}\sum_{n=0}^{\infty}\frac{\sin\left[\frac{\pi}{L}\left(n+\frac{1}{2}\right)x\right]}{(2n+1)(\omega^2+\kappa_n^2)} \times [(\alpha\kappa_n+\omega^2)\sin(\omega t)+\omega(\kappa_n-\alpha)\cos(\omega t)], \tag{5}$$

where $\kappa_n=\alpha+D\frac{\pi^2}{L^2}(n+\frac{1}{2})$.It is easy to see that this is a harmonic signal with the frequency ω everywhere in the string. The amplitude A_L of that signal at $x=L$ related to that at $x=0$ (which is equal A) is defined by

$$\frac{A_L}{A} = \left(\left(1-\frac{4}{\pi}\sum_{0}^{\infty}\frac{(-1)^n(\alpha\kappa_n+\omega^2)}{(2n+1)(\omega^2+\kappa_n^2)}\right)^2 + \left(\frac{4}{\pi}\sum_{0}^{\infty}\frac{(-1)^n(\alpha-\kappa_n)\omega}{(2n+1)(\omega^2+\kappa_n^2)}\right)^2\right)^{1/2} \tag{6}$$

The curve with circle markers in Fig. 1(b) shows the approximation of the analytical relation (6) to the chain of length $N=11$. This curve corresponds to the frequency of the first major harmonic in the power spectrum of the oscillatory BVdP element (see Fig. 2). As far as this harmonics is by far prevailing all the others, then theoretical approach fits the simulations rather well. Note that for high values of the coupling $d>0.5$ the amplitude of oscillations of the BVdP element decreases due to the interaction with the passive elements. This effect cannot be described with Eq. (4). That is why the analytical and numerical curves diverge there. Apart from this, it is obvious that the relation A_{11}/A_1 tends to 1 for large values of coupling. It is illustrated in the inset (b) Fig. 1(b). Note that a saturation in this case takes place for extremely large d which is unphysical in real cardiac cells. The inset (a) in Fig. 1(b) presents the analytical dependence of A_L/A on the frequency of signal ω. It has the form of low-frequency filter and confirms our previous results with the filtering of the complex power spectrum of the BVdP element when it propagates through the passive medium. This finishes our studies of signal propagation through the passive

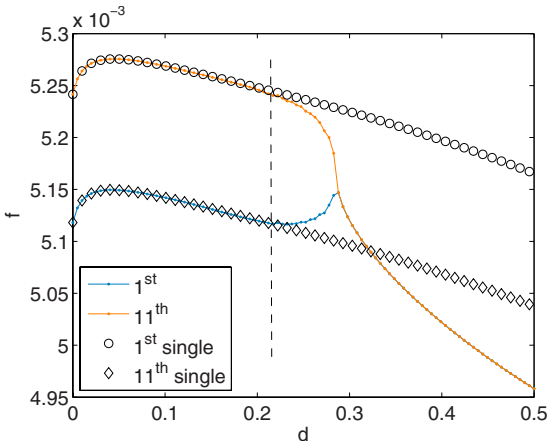

FIG. 3. (Color online) Synchronization of two oscillatory BVdP elements with $a_0=0$ and $a_{11}=0.25$ through the passive chain of nine elements. Two curves with circle and diamond markers shows the frequencies of oscillators in case they were single oscillatory elements in the chain (see text). Two curves with dot markers present the frequencies of two oscillators depending on d (lower dot curve corresponds to the first element). Synchronization sets in for $d \approx 0.22$ and at the approximately average frequency.

medium. In the next subsection we investigate synchronization in such systems.

B. Synchronization of two oscillatory elements through a passive medium

In this subsection the system in question has the same structure as in the previous case except that on the other end of the chain there is another oscillatory BVdP element with a different value of the parameter a.

$$\dot{x}_1 = x_1 - x_1^3/3 - y_1 + d(x_2 - x_1),$$

$$\dot{y}_1 = \varepsilon(x_1 + a_1),$$

$$\dot{x}_i = -\alpha(x_i - P) + d(x_{i-1} - 2x_i + x_{i+1}),$$

$$\overline{i = 2, N-1}, \quad x_{N+1} = x_N,$$

$$\dot{x}_N = x_N - x_N^3/3 - y_N + d(x_{N-1} - x_N),$$

$$\dot{y}_N = \varepsilon(x_N + a_N). \tag{7}$$

We are interested in a phase-synchronized regime between these two oscillatory elements, i.e., the equality of their average frequencies. Simulations were performed for $N=11$, $a_0=0$ and $a_{11}=0.25$, while d was varied. After 50 000 time units skipped for transients, the frequencies were calculated as the average number of oscillations on the interval of 150 000 time units. The frequencies of the two oscillators in dependence on the coupling d are shown in Fig. 3 (two curves with dot markers). Two black curves presented on the same figure by circle and diamond markers show the dependency of the oscillator frequencies on the coupling d in the case of no other oscillatory element on the opposite end of the chain. In other words these curves show how the frequency of the single oscillatory BVdP element is affected by the pure influence of the passive chain. Thus, these changes in frequency have nothing to do with the interaction between the two oscillatory elements. From Fig. 3 we can infer that there exists such a range of coupling values from 0 to approximately 0.22 (dashed line) where the two oscillatory elements interacting through the passive chain almost do not "feel" each other. This follows from the fact that for these values of d the circles and diamonds in Fig. 3 coincide with the dotted lines for the elements with $a_0=0$ and $a_{11}=0.25$, respectively, i.e., there is no visible difference in the frequency of the oscillation from the case of the single oscillatory element in the chain. That is why one can conclude that there exists some threshold value of d_t^i where the interaction starts. The existence of d_t^i is easy to explain, since the amplitude of the signal generated by each oscillatory element increases on the other end of this chain starting from zero and according to the law shown in Fig. 1(b). This amplitude should exceed some critical value to make the interaction possible.

The more interesting effect presented in Fig. 3 concerns the frequency of synchronization. Considering the curves in the figure right to the dashed vertical line one can see that the frequencies of the oscillators tend to approach each other. One unpredictable point is that the two elements synchronize not at the highest frequency of the first oscillator as it should be in case of two interacting nonlinear oscillatory systems but approximately at the average frequency. This is similar to the case of two quasiharmonic oscillators in spite of the fact that the elements in our simulations are essentially nonlinear. The explanation of this effect follows directly from the results presented in the previous section in Fig. 2. There we demonstrated that the signal propagating through the passive element chain is being filtered and thus may be considered as quasiharmonic (see the upper inset in Fig. 2). That is why highly nonlinear oscillators separated by the passive medium affect each other by the quasiharmonic force stipulating for the particular kind of synchronization shown in Fig. 3. Note that the property of filtering is valid only for a certain range of coupling values, i.e., if d is too large, higher harmonics will appear in the power spectrum of the signal on the other end of the chain. Thus if the initial frequency mismatch between the oscillatory elements is too large, then it will demand a very strong coupling to synchronize them and consequently nonlinearity cannot be neglected any more. However, a series of numerical simulations was performed taking into account all the possible values of the initial frequency mismatch and the results of it qualitatively repeat the one shown in Fig. 3. Finally, the last point to outline is the significant decrease of the oscillators frequency right after the onset of synchronization. It is interesting to note that for large values of coupling the decrease of the synchronization frequency is nearly linear. We will explain this effect using an equivalent model of DS presented in the following section.

Summing up we underline three important effects: (i) the existence of a threshold value of coupling d_t^i where an interaction among the oscillators starts (ii) synchronization of the

oscillators at the average frequency as in the case of quasiharmonic systems and (iii) rapid decrease of the synchronization frequency with the growth of d. In the following section we construct an equivalent model for such a system using only two oscillatory elements with the special type of coupling that takes into account the peculiarities of the process in question.

C. Equivalent model for DS

In this section we built an equivalent model to the system described by Eq. (7). The equivalence here is understood in a sense of reproducing the main traits of the synchronization in system [Eq. (7)]. First we take into account the linearity of the passive elements. This means the superposition principle is satisfied for them. Thus we can present the dynamics of the second element $x_2(t)$ as the sum of the two signals $x_2(t)=\tilde{x}_2^1(t)+\tilde{x}_2^N(t)$: (i) the first $\tilde{x}_2^1(t)$ is the signal coming from the first element and (ii) the second $\tilde{x}_2^N(t)$ from the last one. Since we are not interested in the dynamics of passive elements, we can write the system of two interacting oscillatory elements as follows:

$$\dot{x}_1 = x_1 - x_1^3/3 - y_1 + d[\tilde{x}_2^1(t) + \tilde{x}_2^N(t) - x_1],$$

$$\dot{y}_1 = \varepsilon(x_1 + a_1),$$

$$\dot{x}_N = x_N - x_N^3/3 - y_N + d[\tilde{x}_{N-1}^N(t) + \tilde{x}_{N-1}^1(t) - x_N],$$

$$\dot{y}_N = \varepsilon(x_N + a_N), \tag{8}$$

where $x_{N-1}(t)=\tilde{x}_{N-1}^N(t)+\tilde{x}_{N-1}^1(t)$ similarly to the second element. We now can regroup the coupling term into two parts with different physical notations. For the first element it looks like $d[\tilde{x}_2^1(t)+\tilde{x}_2^N(t)-x_1]=d\{[\tilde{x}_2^1(t)-x_1\}+d\tilde{x}_2^N(t)$. The first term here describes the influence of the whole passive chain on the first element as if there is no other oscillator on the other end. This influence produces changes in the individual frequencies of the oscillator with the increase of d (see curves with circle and diamond markers in Fig. 3). We will neglect this term, since we are interested only in synchronization properties of the systems. The second term of coupling $d\tilde{x}_2^N(t)$ represents the signal coming from the other oscillator. It is responsible for synchronization. Note that according to the previous results this signal also depends on d (frequency filtering and amplitude dependency). Thus the equivalent system for DS in the chain may be written as

$$\dot{x}_1 = x_1 - x_1^3/3 - y_1 + d\tilde{x}_2^N(t,d),$$

$$\dot{y}_1 = \varepsilon(x_1 + a_1),$$

$$\dot{x}_N = x_N - x_N^3/3 - y_N + d\tilde{x}_{N-1}^1(t,d),$$

$$\dot{y}_N = \varepsilon(x_N + a_N), \tag{9}$$

Now we need to specify $\tilde{x}_2^N(t,d)$ and $\tilde{x}_{N-1}^1(t,d)$ in terms of the variables x_N, y_N and x_1, y_1, respectively. To do this let us mark that the passive chain may be considered as an integrating chain. Indeed applying Laplace transform to the equation $\dot{x}=-\alpha x$ for the passive element, then its transmission gain is defined by the relation,

$$K(\omega) = \frac{\alpha}{\alpha + i\omega}, \tag{10}$$

which is the gain of the low-frequency filter or integrator. This means that the signal $x_N(t)$ going through the passive medium is being integrated with respect to time. However according to the relation $\dot{y}_N=\varepsilon(x_N+a_N)$ we can state that integrating gives with the change of variables $y_N(t)$. Thus far we considered only the filtering property of the passive chain. Taking into account the amplitude dependency $A(d)$ described by Eq. (6), we obtain finally (the index N is substituted by 2 for convenience),

$$\dot{x}_1 = x_1 - x_1^3/3 - y_1 + dA(d)y_2,$$

$$\dot{y}_1 = \varepsilon(x_1 + a_1),$$

$$\dot{x}_2 = x_2 - x_2^3/3 - y_2 + dA(d)y_1,$$

$$\dot{y}_2 = \varepsilon(x_2 + a_2). \tag{11}$$

The amplitude of the oscillation of the x variable of $BVdP$ oscillator is three times larger than the y variable that is why the amplitude dependence $A(d)$ should be scaled by factor 3. Numerical simulations of system [Eq. (11)] for the values of parameters $a_1=0$ and $a_2=0.25$ give the results presented in Fig. 4. Here one can see the dependency of the oscillation frequencies of both elements on the coupling parameter d. Since we have neglected term $\tilde{x}_2^1(t)-x_1$ in Eq. (8) we do not observe any changes in the frequency of oscillators caused by their interaction with passive elements. The inset in the figure illustrates the dependency of the ratio f_1/f_2 of the oscillator frequencies on d. It is easy to see that there is a range of values of coupling from 0 to about 0.18 (dashed vertical line) where the oscillators almost do not interact, i.e., the ratio f_1/f_2 does not change for d growing from 0 to 0.18. Apart from this, synchronization in this system occurs exactly at the average frequency of the two elements. And finally a drastic decrease of the frequency with the increase of

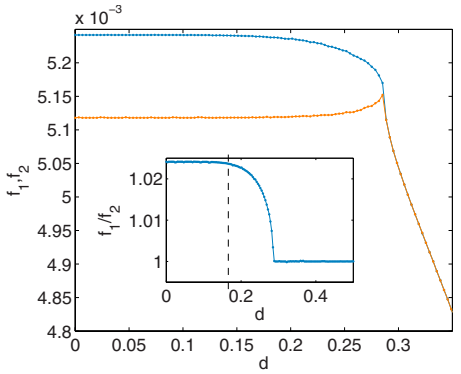

FIG. 4. (Color online) Synchronization in the equivalent model of DS. Two curves are the frequencies of oscillators depending on d. Inset illustrates the f_1/f_2 ratio.

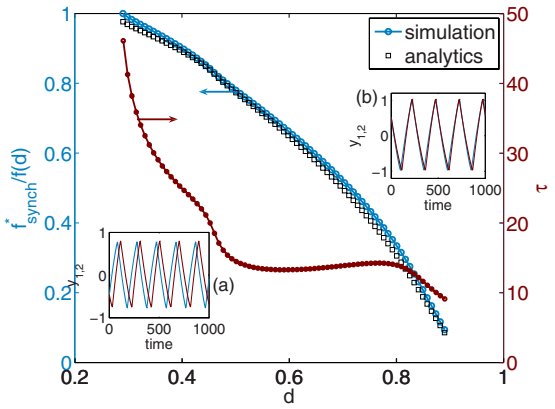

FIG. 5. (Color online) Effect of the frequency decrease in the equivalent model of DS. Solid blue curve with circle markers (using left ordinate axes) presents the dependency of frequency scaling $f^*_{synch}/f(d)$ on coupling strength obtained numerically. Black squares are analytical approximation (13) of $f^*_{synch}/f(d)$. Dark red curve with circle markers (using right ordinate axes) is the dependency of time shift τ between two synchronous time series of the y variable of the oscillators on d. Insets show the characteristic time series of the synchronous motions of two oscillators for $d=0.29$ (a) and $d=0.5$ (b).

coupling right after the onset of synchronization is also observed. These three points mean that our equivalent model reproduces all of the underlined previously effects.

Now we concentrate on the effect of frequency decrease because it is significant in a large range of coupling. We will explain the phenomenon using our equivalent model of DS. First we notice that synchronization that sets in at $d\approx 0.29$ (Fig. 4) is in-phase with some phase shift which vanishes with the increase of the coupling strength. This fact is supported by the two time series of the process for $d=0.29$ (right after the onset of synchronization) and $d=0.5$ that are presented in Fig. 5 in the insets (a) and (b), respectively. The time delay τ between the two elements is clearly seen in the inset (a), while both realizations are almost identical for $d=0.5$ [inset (b)], i.e., $\tau=0$. Thus, in order to describe the frequency decrease, we make the assumption that after synchronization sets in we have $y_2(t)\approx y_1(t-\tau)$. Second, we suppose that τ is small enough, such that $\dot{y}_1(t)\approx[y_1(t)-y_1(t-\tau)]/\tau$. Hence, substituting $y_2(t)=y_1(t)-\tau\dot{y}_1(t)$ into the first equation of system [Eq. (11)], we obtain the system governing the dynamics, for example, of the first element in the synchronous regime,

$$\dot{x} = \xi x - x^3/3 - y,$$

$$\dot{y} = \bar{\epsilon} x. \tag{12}$$

where $y=[1-dA(d)]y_1$, $\xi=[1-dA(d)\tau\epsilon]$, $\bar{\epsilon}=[1-dA(d)]\epsilon$, and $a=0$ as it was in simulations for the first elements. Supposing that system [Eq. (12)] spends most time on the curve of slow motions $\xi x-x^3/3-y=0$ and moves immediately from one stable brunch of this curve to another, one can integrate the equations and find the frequency of the oscillations,

$$f = \frac{\bar{\epsilon}}{2\xi(3/2+\ln 1/2)} = f_0\frac{1-dA(d)}{1-dA(d)\tau\epsilon}, \tag{13}$$

where $f_0=\epsilon/2(3/2+\ln 1/2)$ is the individual frequency of the oscillator. Thus we get the desired scaling $f^*_{synch}/f(d)$ of the frequency right in the moment of the onset of synchronization to the frequency of synchronous oscillations of two elements depending on d. Numerical dependency of $f^*_{synch}/f(d)$ on coupling strength is shown in Fig. 5 by the solid line with circle markers (using the left ordinate axes). In order to compare analytical solution (13) with this curve, we have to take into account the dependence of the time delay τ on the coupling d which is presented in Fig. 5 by the dark red curve with circle markers (using the right ordinate exes). Incorporating this dependency into Eq. (13), we obtain finally an analytical scaling $f^*_{synch}/f(d)$ presented in Fig. 5 by black squares. One can see that our theoretical approximation fits rather well to the numerical simulations. Various divergences between the analytical and numerical curves may be explained by some idealizations made: (i) smallness of τ, (ii) immediate movement of the system between the branches of the curve of slow motions.

In the end of this section we draw the attention to the fact that the effect of the significant frequency decrease described by the scaling [Eq. (13)] is due to the frequency filtering property of the passive medium, because only in this case the equivalent model of DS [Eq. (11)] is valid.

III. DS IN BIOLOGICALLY RELEVANT MODELS

As mentioned in the introduction, the current task appears from experiments with cardiac cell culture. Thus far we considered simple phenomenological models only. However to prove the generality of the results obtained as well as to support the possibility of application of the results to cardiac biology, we perform similar studies with biologically relevant models. The following two subsections describe models of cardiomyocite and fibroblast. After that the results of simulations of these models are presented.

A. Luo-Rudy phase I model of cardiac cell

As a model of cardiac myocite we use the well known Luo-Rudy phase I model [19]. This model is of Hodgkin-Huxley [20] type and includes eight nonlinear ordinary differential equations to describe the dynamics of a single cardiac cell. The main equation governs the dynamics of the cell membrane voltage V measured in millivolts,

$$C_m\frac{dV}{dt} = -I_{ion} + I^{ext}, \tag{14}$$

where $C_m=1$ μF/cm^2 is the membrane capacity. The time unit of the model is 1 ms. I^{ext} is a constant external electrical stimulus and I_{ion} is a sum of six ionic currents flowing through the membrane,

$$I_{ion} = I_{Na} + I_{si} + I_K + I_{K1} + I_{Kp} + I_b, \tag{15}$$

where I_{Na} is a sodium current, I_{si} slow inward calcium current, I_K potassium current, I_{K1} stationary potassium current,

I_{Kp} plateau potassium current and I_b a background current. These currents are measured in $\mu A/cm^2$ and defined by

$$I_{Na} = G_{Na} \cdot m^3 hj \cdot (V - E_{Na}),$$

$$I_{si} = G_{si} \cdot df \cdot [V - E_{si}(V,c)],$$

$$I_K = G_K \cdot xx_i(V) \cdot (V - E_K),$$

$$I_{K_1} = G_{K1} \cdot k_{1i}(V) \cdot (V - E_{K1}),$$

$$I_{K_p} = G_{Kp} \cdot k_p(V) \cdot (V - E_{K1}),$$

$$I_B = G_b \cdot (V - E_b). \quad (16)$$

Here G_q and E_q for $q \in \{Na, si, K, K1, Kp, b\}$ denote, respectively, the maximal conductance and the reversal potential of the corresponding ionic current. Each of the gating variables $g_i \in \{m, h, j, d, f, x\}$, $i = 1, \ldots, 6$ is described by the ordinary differential equation,

$$\dot{g}_i = \alpha_{g_i}(V)(1 - g_i) - \beta_{g_i}(V) g_i. \quad (17)$$

Nonlinear functions $\alpha_{g_i}(V)$ and $\beta_{g_i}(V)$ as well as $E_{si}(V,c)$, $x_i(V)$, $K_{1i}(V)$, $K_p(V)$ are fitted to the experimental data [19]. The dynamics of the external concentration of calcium ions is given by the first order differential equation,

$$\dot{c} = 10^{-4} I_{si}(V,d,f,c) + 0.07(10^{-4} - c). \quad (18)$$

When I^{ext} is equal to zero, the cell described by this model demonstrates excitable behavior. On the other hand we need to simulate an oscillatory cardiac cell in our task. It is shown in [14] that the excitable Luo-Rudy cell can be turned into an oscillatory regime by adding the depolarizing constant external current I^{ext}. It was also shown that at the value of $I^{ext} \approx 2.21$ a stable limit cycle in this model appears via saddle-node homoclinic orbit bifurcation. When $I^{ext} > 2.21$ its value also defines the frequency of the oscillation similarly to the parameter a in the BVdP system.

B. Sachse model of cardiac fibroblast

To simulate cardiac fibroblast we use the model proposed by Sachse *et al.* in [21]. This model is of the same type as the Luo-Rudy model. It involves three ionic currents to describe the voltage of a single cell,

$$C_m \dot{V}_f = -(I_{Kir} + I_{Shkr} + I_b). \quad (19)$$

The inwardly rectifying current I_{Kir} is given by

$$I_{Kir} = G_{Kir} O_{Kir} \sqrt{[K^+]_0} (V_f - E_K). \quad (20)$$

Here G_{Kir} is the maximal conductance for this current and E_K is the reversal potential. The probability O_{Kir} of the channel to be opened is defined as

$$O_{Kir} = \frac{1}{\alpha_{Kir} + \exp(\beta_{Kir}(V_f - E_K)F/RT)}, \quad (21)$$

where α_{Kir} and β_{Kir} are constants, F is the Faraday constant, R is the gas constant and T is the temperature.

The outward current I_{Shkr} is time and voltage dependent. In [21] it was reconstructed based on the Goldman-Hodgkin-Katz current equation and a Markovian model of the delayed rectifier K^+ currents,

$$I_{Shkr} = P_{Shkr} O_{Shkr} \frac{V_f F^2}{RT} \frac{[K^+]_i - [K^+]_0 \exp(-V_f F/RT)}{1 - \exp(-V_f F/RT)},$$

with the permeability P_{Shkr}. The Markovian model describes five closed states, $C0_{Shkr}, \ldots, C4_{Shkr}$ and one open state O_{Shkr},

$$\dot{C}0_{Shkr} = -4k_v C0_{Shkr} + k_{-v} C1_{Shkr},$$

$$\dot{C}1_{Shkr} = 4k_v C0_{Shkr} - (3k_v + k_{-v}) C1_{Shkr} + 2k_{-v} C2_{Shkr},$$

$$\dot{C}2_{Shkr} = 3k_v C1_{Shkr} - (2k_v + 2k_{-v}) C2_{Shkr} + 3k_{-v} C3_{Shkr},$$

$$\dot{C}3_{Shkr} = 2k_v C2_{Shkr} - (k_v + 3k_{-v}) C3_{Shkr} + 4k_{-v} C4_{Shkr},$$

$$\dot{C}4_{Shkr} = k_v C3_{Shkr} - (k_0 + 4k_{-v}) C4_{Shkr} + k_{-0} O_{Shkr},$$

$$\dot{O}_{Shkr} = k_0 C4_{Shkr} - k_{-0} O_{Shkr}.$$

Here the rate coefficients k_v and k_{-v} are exponential functions of voltage and k_0, k_{-0} are constants.

The background current I_b is defined simply as

$$I_b = G_b(V_f - E_b). \quad (22)$$

All in all the Sachse model of fibroblast is described by seven dynamical variables and seven nonlinear ODEs.

C. Signal propagation properties

In this subsection we simulate a chain of fibroblasts with the only oscillatory cardiac cell at the end of it. We are interested in the properties of signal propagation in this system especially with respect to our previous results obtained for the BVdP model. A chain of $N=11$ elements is considered. The value of the external current for the cardiomyocite I^{ext} was equal 3, 2.8, and 2.6. Figure 6 illustrates what amplitude has the signal in the last element of the chain if it is generated by the oscillatory Luo-Rudy element at the other end of the chain. The inset in the figure shows the distribution of the amplitudes over the elements for a fixed value of $d = 0.05; 0.03; 0.01$. Comparing these curves with Fig. 1, one can see that the chain of real fibroblast demonstrates qualitatively the same behavior as the phenomenological chain, namely, a drastic decrease of the oscillation amplitude over the distance and a monotonic increase of the amplitude in the last element with growing d. Figure 7 demonstrates the frequency filtering property of the fibroblast chain. The main plot shows the power spectrum of the oscillatory Luo-Rudy element being at the end of the chain. This spectrum has at least five distinct harmonics. The largest at about 1.4 Hz corresponds to the frequency of periodic oscillations of the action potential and all the others form a nonlinear profile of the cardiac action potential. Note that in contrast to a BVdP

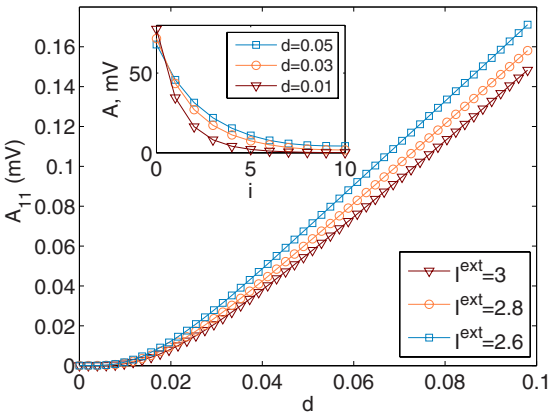

FIG. 6. (Color online) The dependencies of the oscillation amplitude of the last passive element A_{11} related to that of the first oscillatory element A_1 on the coupling d for different values of $I^{ext}=3;2.8;2.6$ (squares, circles, triangles). In the inset there is a distribution of oscillation amplitudes over the chain for fixed values of coupling $d=0.05;0.03;0.01$ (squares, circles, triangles).

element, the cardiomyocite exhibits a time series which is not symmetric with respect to zero. Thus its power spectra has also a large zero frequency component corresponding to constant shift of the time series. This component is not presented in Fig. 7 for clearness of the plot. The lower and upper insets in Fig. 7 show the power spectra of the fifth and 11th elements in the chain, respectively. One can see that the signal at the other end of the chain (upper inset) possess the only significant component at the frequency of periodic oscillations of the cardiomyocite and thus this signal is quasiharmonic there. Comparing these results with Fig. 2 it is easy to see that the chain of fibroblasts described by the sophisticated biologically relevant model demonstrates the same frequency filtering property as the chain of linear passive units.

The results of the current subsection show that the chain of fibroblasts simulated by a biologically relevant model exhibits the same main properties of signal propagation as our phenomenological one. Namely, two major effects are observed in both models: (i) lowering of the signal amplitude, while it propagates through the fibroblast medium and (ii) power spectrum filtering responsible for quasiharmonics profile of oscillations at the end of the chain.

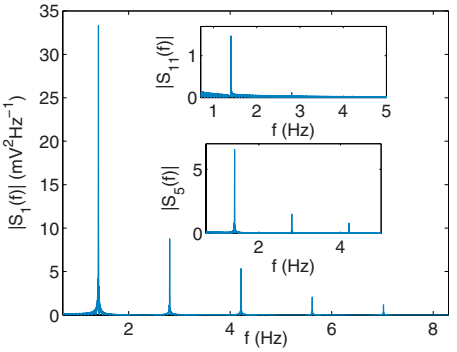

FIG. 7. (Color online) The power spectrum of the voltage variable time series of the elements of the chain obtained by fast Fourier transform for $d=0.05$. Lower and upper insets show power spectrum of the fifths and last elements of the chain, respectively.

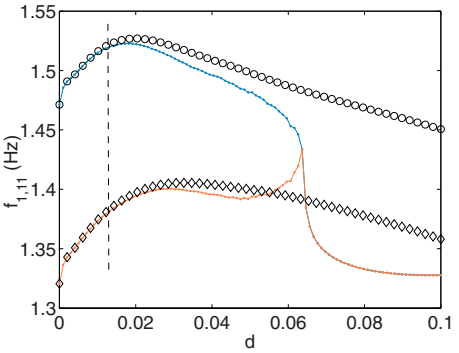

FIG. 8. (Color online) Synchronization of two oscillatory Luo-Rudy elements with $I_1^{ext}=2.8$ and $I_{11}^{ext}=3$ through the fibroblast chain of nine elements. Two curves with circle and diamond markers shows the frequencies of oscillators in case they were single oscillatory elements in the chain (see text). Two curves with dot markers present the frequencies of two oscillators depending on d (lower dot curve corresponds to the first element). Synchronization sets in for $d\approx 0.063$ and at the approximately average frequency.

D. Synchronization of two cardiomyocites through the fibroblast chain

The chain of $N=11$ elements was simulated. The first and the last units of the chain are oscillatory Luo-Rudy elements with $I_1^{ext}=2.8$ and $I_{11}^{ext}=3$. Figure 8 shows synchronization phenomena occurring in the system. As in the case of the phenomenological models (Fig. 3), two black curves with circle and diamond markers represent the frequencies of the oscillatory cells depending on the coupling d in the case of the only oscillatory cell in the chain. One can see that the influence of the fibroblast chain on a single oscillatory cardiac cell produces the dependency of its frequency on the coupling of the same kind as for the BVdP model. The curves with dot markers in Fig. 8 show the frequencies of oscillatory cardiomyocites interacting through the fibroblast chain. Three main effects are observed again: (i) the existence of a threshold value of coupling (dashed vertical line in the figure) where the interaction begins (ii) synchronization at the average frequency that is characteristic for quasiharmonic oscillators and (iii) a drastic decrease of the synchronization frequency with growing d. Concluding this section we state that synchronization in biologically relevant models appear in the same way as in phenomenological models of cardiac cell and exhibits the same significant peculiarities.

IV. DS IN 2D MEDIUM

This section generalizes previous results to the case of nonhomogeneous ensembles of oscillatory cardiac cells interacting through a two-dimensional passive medium of fibroblasts. Simulations were performed with a 60×60 lattice of cardiac cells described by the Luo-Rudy and Sachse models. The structure of the system is shown in Fig. 9. Here white space corresponds to a passive fibroblast medium with resting potential −60 mV and colored areas represent nonidentical clusters of oscillatory cardiac cells. The color gradation reflects the value of the parameter I_{ij}^{ext} for each oscillatory cell, i.e., reflects the individual frequencies of

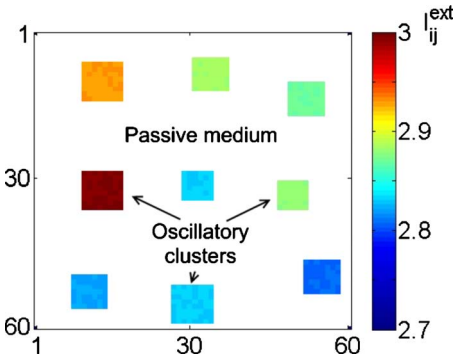

FIG. 9. (Color online) Topology of the experiment. White spaces correspond to the fibroblast medium. Colored areas represent oscillatory clusters. Color gradation reflects individual frequencies of cardiac pacemakers.

pacemakers. One can see that there nine clusters are formed which are arranged randomly in the lattice. There is a random variation of the cluster size from 6×6 to 9×9 elements. Each cluster has its average individual frequency defined by the average I^{ext} parameter value chosen randomly from the range [2.8;3]. Apart from this, a small variation of I^{ext} (up to 0.005) within each cluster also exists. Such topology follows also from biological experiments [13] and qualitatively reproduces their conditions. The whole system was simulated for 6×10^6 where 4.5×10^6 ms were skipped for transients and 1.5×10^6 ms were used for frequencies calculation. Figure 10 demonstrates the dependencies of the average cluster frequencies f_i on the coupling strength d. Although synchronization in this case is much more complex, some characteristic traits still persist. Thus, the red circles in Fig. 10 outline the places where synchronization sets in at the average frequency of interacting units. Second, at large scales of d the frequencies of oscillatory ensembles behave similarly to that of two interacting cells (Fig. 8), i.e., a slight increase of the frequencies for small couplings and consequent decrease as the d growths are observed. Additionally, global synchronization occurring at $d\approx0.47$ appears after several regimes of cluster synchronization, e.g., for

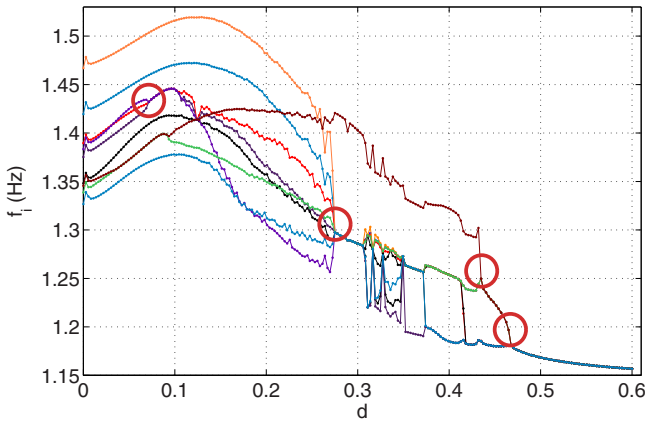

FIG. 10. (Color online) Average frequencies of oscillatory ensembles depending on coupling strength d. Red circles shows the places where the characteristic traits of DS are observed. Global synchronization sets in via set of clustered regimes.

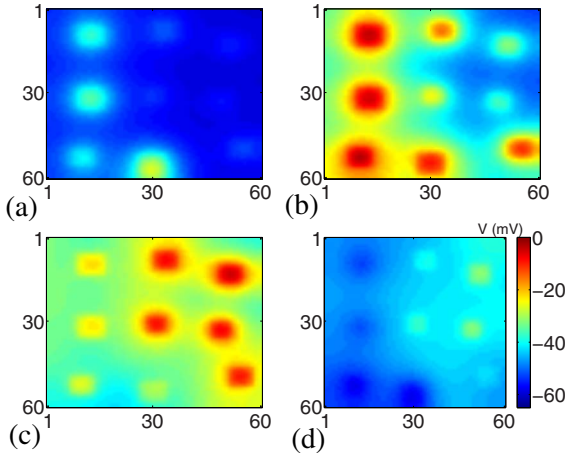

FIG. 11. (Color online) Snapshots of the lattice cell voltage V_{ij} after transients for different time moments: (a) 0 ms, (b) 30 ms, (c) 60 ms, (d) 90 ms. One can see a wave propagating from down left corner of the lattice in right-upward direction.

$d=0.3;0.45$ two clusters of synchronization are observed and for $d=0.4$ there are three of them. Finally, we note that due to the high complexity and inhomogeneity of the system, there are region of couplings were an intricate dynamics is demonstrated. For example for $d\in[0.31;0.35]$ where one synchronous cluster splits into two the frequencies of the oscillatory ensembles show a complex interplay that may be caused by the finiteness of calculation time and long transient processes at the border of two regimes.

The last thing to note is that the regime of global synchronization is represented by the target wave that spreads in the system (Fig. 11). Due to the fact that fibroblasts do not produce action potential their oscillations have very small amplitudes such that one observe a wave as the consequence of periodic excitations of oscillatory clusters with a fixed phase shift.

V. SPATIAL SCALING OF DS

In this section we present a general framework of finding scalings of DS properties, namely, synchronization threshold d_s and synchronization frequency f_s, with a varying size of the passive medium between the oscillators. Here we consider a chain of N passive elements described by Eq. (2) and two oscillatory BVdP elements with different individual frequencies ($a_1=0$; $a_2=0.25$) at the ends of the chain. We vary the number of passive units N between the oscillators and calculate the threshold value of coupling strength d_s when synchronization sets in. Figure 12(a) shows the dependency of the relation $\sqrt{d_s/d_1}$ on N where d_1 is the synchronization threshold in case of a single passive element in the chain. This dependency turned out to be linear implying the quadratic power law scaling for the synchronization threshold d_s with respect to passive elements number N. Numerically obtained scaling of the frequency of the synchronization f_s, i.e., the frequency of oscillations right after synchronization sets in, is presented in Fig. 12(b) by the curve with square markers. According to our previous results synchronization occurs

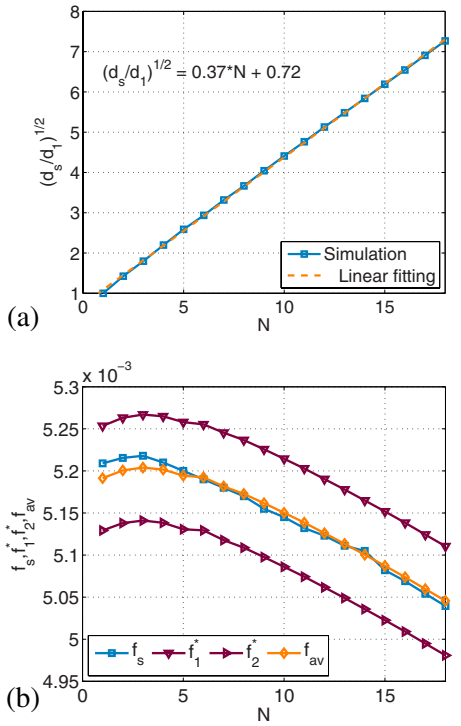

FIG. 12. (Color online) (a) Spatial scaling of threshold coupling strength d_s for which synchronization sets in for the chain of N passive units separating two BVdP elements. The relation $\sqrt{d_s/d_1}$ obtained in simulation is fitted by the linear approximation implying power law dependency. (b) Scaling of synchronization frequency f_s (square markers curve) obtained numerically and f_{av} (diamond markers curve) obtained from the general framework of finding DS characteristics from scaling properties (see text).

at the average frequency of the two elements. However one should take into account the impact of the passive elements on the individual frequency of the oscillator. That means that the frequency of a single oscillatory element coupled with the chain of passive units is a function of two variables $f^*=f^*(d,N)$. In our case of a BVdP element the characteristic kind of that function is shown in Fig. 13. One peculiarity which is worth noticing is that for large numbers N (e.g., $N \gtrsim 16$ in Fig. 13) the frequency of the oscillator depends on d only. Having obtained such a kind of dependency for the individual frequency of an oscillator, one can do the following: (i) for each number of passive elements N and for each corresponding threshold coupling strength d_s [Fig. 12(a)] we can find the values of the individual frequencies $f_1^*(d_s,N)$; $f_2^*(d_s,N)$ for both oscillators with $a_1=0$; $a_2=0.25$, respectively. These two dependencies are presented in Fig. 12(b) by the curves with triangle markers. Their average value $f_{av}=(f_1^*+f_2^*)/2$ is shown in the same figure by the curve with diamond markers and fits to the previously numerically obtained results for the synchronization frequency f_s rather well, thus, confirming that DS takes place at the average frequency of oscillators similarly to the quasiharmonic system. Summarizing this section we present a general workflow for finding DS characteristics for an arbitrary number of passive elements N,

(i) find the synchronization threshold d_1 for the case of single passive element between the oscillators;

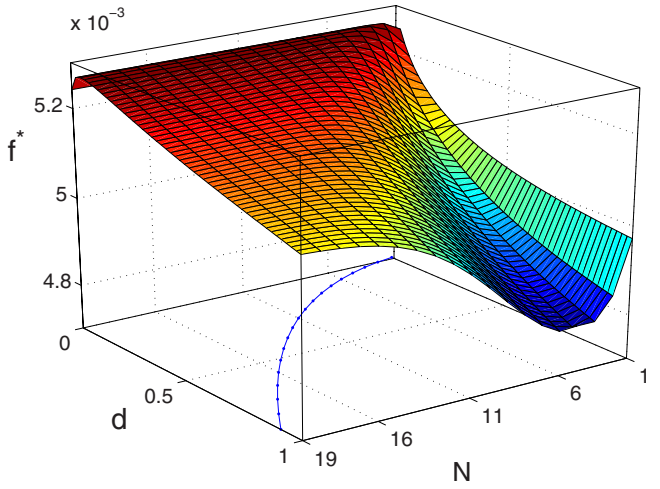

FIG. 13. (Color online) The dependency of individual frequency of the BVdP oscillator with $a=0$ interacting with the passive chain of size N with coupling strength d. Blue curve with dot markers is the threshold coupling strength d_s scaling which is used in order to find f_1^* and f_2^* (see text).

(ii) find the individual frequency dependencies $f^*(d,N)$ for a single oscillatory element coupled with the passive chain (Fig. 13);

(iii) for chosen N use the quadratic power law scaling [Fig. 12(a) to find the synchronization threshold d_s (curve with dot markers in Fig. 13);

(iv) find the synchronization frequency from the relation $f_s=[f_1^*(d_s,N)+f_2^*(d_s,N)]/2$;

(v) scaling of f_s for a chosen N with respect to further increase of the coupling d satisfies the relation (13).

VI. CONCLUSION

In this paper the effect of distant synchronization of oscillatory elements through a passive medium was considered. The main mechanisms responsible for this phenomenon are discussed and three characteristic features of the process are outlined, namely: (i) for such kind of synchronization there exists some threshold value of coupling between the elements where the interaction between the oscillators sets in (ii) synchronization takes place at the average frequency of oscillators which is customary for quasiharmonic elements and (iii) a rapid decrease of the synchronization frequency with the growing d. First two features are explained by studying of the signal propagation through a passive medium. As for the first point, the existence of a threshold coupling value is caused by a continuous increase of the signal amplitude from zero. If there is a finite frequency mismatch between the oscillators, then it will demand a finite amplitude of the signal which is responsible for their interaction and, thus, some critical value of coupling is to be achieved to satisfy this requirement. The second feature of DS is caused by the frequency filtering property of the passive medium providing a quasiharmonic interaction between the nonlinear oscillators. One should take into account that this property is held for a certain value of coupling only, i.e., if the coupling

is too large the higher harmonics in the power spectrum of the signal will appear in the output. Hence, too large frequency mismatch between the oscillators demanding a large coupling for the synchronization to set in consequently involves the nonlinearity in the interaction and changes the scenario of the process.

We also proposed an equivalent model describing DS in a chain. This model reproduces qualitatively all main features of DS observed in the numerical simulation. Using this model we explained the effect of frequency decrease after synchronization onset and derived an analytical scaling of the frequency which rather well fits to the simulations.

These results were generalized to the case of a two-dimensional medium. Synchronization of nonidentical oscillatory clusters of cardiac cells through the passive medium of fibroblast was shown to demonstrate characteristic traits of DS studied in chains.

DS was considered in both phenomenological and more realistic and biologically motivated models of cardiac cells. The results can be used to explain experimental observations of synchronization of oscillatory cardiomyocites separated by a fibroblast medium [13].

We also presented a general framework of finding the DS characteristics for an arbitrary number of passive elements using scaling dependencies for threshold coupling strength and for the synchronization frequency. Application of this framework was presented for a chain of two BVdP oscillators interacting through passive units.

ACKNOWLEDGMENTS

We acknowledge support from the Federal Program "Scientific and Scientific-educational brainpower of innovative Russia" for 2009–2013 (Contract Nos. П2018, П15, П2308, 02.740.11.5138, П942, and 02.740.11.5188), and from the RFBR (Grant Nos. 08-02-92004, 08-02-970049, and 10-02-00940).

[1] A. S. Pikovsky, M. G. Rosenblum, and J. Kurths, *Synchronization: A Universal Concept in Nonlinear Sciences* (Cambridge University Press, Cambridge, 2001).
[2] G. V. Osipov, J. Kurths, and Ch. Zhou, *Synchronization in Oscillatory Networks* (Springer-Verlag, Berlin, 2007).
[3] G. Bub, A. Shrier, and L. Glass, Phys. Rev. Lett. **88**, 058101 (2002).
[4] J. P. Fahrenbach, R. Mejia-Alvarez, and K. Banach, J. Physiol. (London) **585**, 565 (2007).
[5] M. R. Tinsley, A. F. Taylor, Z. Huang, and K. Showalter, Phys. Rev. Lett. **102**, 158301 (2009).
[6] H. Daido and K. Nakanishi, Phys. Rev. Lett. **93**, 104101 (2004).
[7] G. Bub, A. Shrier, and L. Glass, Phys. Rev. Lett. **94**, 028105 (2005).
[8] J. H. E. Cartwright, Phys. Rev. E **62**, 1149 (2000).
[9] A. Sherman and J. Rinzel, Biophys. J. **59**, 547 (1991).
[10] J. N. Weiss, A. Garfinkel, H. S. Karagueuzian, Zh. Qu, and P.-S. Chen, Circulation **99**, 2819 (1999).
[11] V. S. Petrov, G. V. Osipov, and J. A. K. Suykens, Phys. Rev. E **79**, 046219 (2009).
[12] M. Miragoli, N. Salvarini, and S. Rohr, Circ. Res. **101**, 755 (2007).
[13] W. Chen, S. C. Cheng, E. Avalos, O. Drugova, G. Osipov, P.-Y. Lai, and C. K. Chan, EPL **86**, 18001 (2009).
[14] A. K. Kryukov, V. S. Petrov, L. S. Averyanova, G. V. Osipov, W. Chen, O. Drugova, and C. K. Chan, Chaos **18**, 037129 (2008).
[15] V. Jacquemet, Phys. Rev. E **74**, 011908 (2006).
[16] K. F. Bonhoeffer, Naturwiss. **40**, 301 (1953).
[17] R. FitzHugh, Bull. Math. Biophys. **17**, 257 (1955).
[18] P. Kohl, A. G. Kamkin, I. S. Kiseleva, and D. Noble, Exp. Physiol. **79**, 943 (1994).
[19] C.-H. Luo and Y. Rudy, Circ. Res. **68**, 1501 (1991).
[20] A. L. Hodgkin, A. F. Huxley, J. Physiol. (London) **117**, 500 (1952).
[21] F. B. Sachse, A. P. Moreno, and J. A. Abildskov, Ann. Biomed. Eng. **36**, 41 (2007).